Scientific Research Communications

Research Article

Sci. Res. Comm. (2024)
Volume 4, Issue 2
doi: 10.52460/src.2024.007

Utilization of Short Span Web-Tapered Beams Using Flexible Nodal Bracing

Fatma Kömürcü[1] Oğuzhan Toğay[1,*]

[1] İzmir Katip Çelebi University, Faculty of Engineering and Architecture, Department of Civil Engineering
[*] Corresponding author: oguzhan.togay@ikc.edu.tr

Received: 14.06.2024 Accepted: 30.07.2024

Abstract

The use of steel structures with varying cross-sectional dimensions along their length is common, with nodal braces playing a critical role in enhancing their load-carrying capacity and stability. These braces distribute loads within the structure and improve resistance to lateral forces. Current design guidelines, such as American Institute of Steel Construction (AISC) Design Guide 25 and AISC 360-22, offer a general framework for elements with fixed brace conditions and prismatic cross-section. This study aims to be a pioneering investigation into the variation of brace force values in short-span and compact web-tapered beams under a single loading condition. The article seeks to comprehensively examine the requirements and limits of brace force in short-span web-tapered compact beams. To achieve this goal, parametric finite element analyses are utilized to explore how brace force changes concerning beam geometry and material properties under a single loading condition. The beam used was considered as doubly symmetric and divided into 100 nodes and supported by a nodal brace at the middle node. The beam is 2540 mm (100 in) long, its depth tapering from 1066.8 mm (42 in) to 924.6 mm (36.4 in) over its span and unbraced length is 1270 mm (50 in). In terms of finite element analysis, the software utilized significantly influences the accuracy and reliability of results, particularly in scenarios involving inelastic nonlinear analysis. In this study, the ABAQUS software was employed specifically to conduct parametric finite element analyses, considering the complexities of inelastic material behavior. Maximum Brace Force value that has been found in the simulation studies has been found as 2.15%. Consequently, the findings of this research are intended to contribute to the development of a new design method for determining the requirements and limits of brace force in short-span, determining required brace stiffness and variable cross-sectional dimension compact beams, to contribute to the safe and economical design of such beams, and to provide engineers with ideas to consider and data to use in their designs.

Keywords: Web-tapered beam; brace; brace force; compact beam; finite element method

1. Introduction

In structural engineering, the design and analysis of steel beams are critical for ensuring safety and efficiency in construction. Steel structures offer significant advantages over other types of structures due to the flexibility of variable cross-section elements and the ability to produce welded sections. One such structural member is the web-tapered section steel members. These

web-tapered sections can be enhanced by the addition of nodal bracing at the mid-section to increase load-bearing capacity and stability. This study focuses on short-span web-tapered compact welded I-section beams that are supported by a flexible nodal brace at the midspan of its top flange. This study was designed in a limited scope to examine the performance of short span beams in the initial phase of the research. It is planned to expand the scope and examine other beam types in future studies.

Miller (2003) highlighted the lack of design equations for web-tapered I-section beams, emphasizing the need for further research in this area, particularly in the inelastic range using nonlinear finite element analysis. Also, the author mentioned that behavior of web-tapered I-shaped beams at the ultimate stage may be determined by a number of variables, including the flange width, flange thickness, web thickness, unbraced length, tapering angle, etc., according to the results of the current parametric research. The author also showed in his study that the plate slenderness ratios in the American Institute of Steel Construction (AISC) 360-22 (2022) Load and Resistance Factor Design (LRFD) Table B4.1 are inadequate for compact beam behavior in adequately braced web-tapered I-shaped beams in order to provide accurate estimates for the elastic buckling resistance. Soltani et al. (2019) examined the lateral buckling of three comprehensive I-beam examples. These included simply supported doubly symmetric I-sections and axially varied materials in both homogeneous and inhomogeneous tapered beams, utilizing a new finite element approach. Soltani and Asgarian (2020) developed a finite element model to assess the lateral-torsional stability of axially functionally graded beams featuring tapered bi-symmetric I-sections under a range of boundary conditions. Asgarian et al. (2013) developed a theoretical and numerical model based on the power series method for beams with arbitrary cross-sections and boundary conditions. Lateral buckling loads were determined by solving the eigenvalue problem of the algebraic system derived from this model. The study compared these results with finite element solutions obtained through established numerical or analytical methods, such as Ansys software, and concluded that the proposed method is effective for analyzing the stability of both tapered beams and beams with constant cross-sections. Mercuri et al. (2020) highlighted that the use of approximate methods becomes necessary due to the complexity of analytical solutions for tapered sections. It is noted that commercial software often fails to accurately account for the features of non-prismatic beams, resulting in inconsistent structural analyses, erroneous stress distribution estimations, and rough predictions of the structural element's strength. In the study, the stiffness matrix was analytically defined for both homogeneous prismatic and tapered beams, and the resulting finite element outcomes were compared with the results obtained from SAP2000 for the same beams. Toğay (2024) examined the inelastic nonlinear buckling analysis with stiffness reduction factors used in web-tapered I sections, compared this analysis with finite element analysis and found a 98.6% agreement. This study emphasized the consistency of inelastic nonlinear buckling analysis especially in fixed-supported web-tapered I sections and the usability of inelastic nonlinear buckling analysis in this field.

Foster and Gardner (2013) used a geometrically and materially non-linear finite element model to conduct a series of experiments on simply supported beams with variations in restraint spacing and stiffness. Authors found that at the minimum required stiffness, restraint forces reached their peak values, but increasing the stiffness beyond this point caused the forces to reduce rapidly and ensured that full capacity of the restrained member was reached. Tankova et al. (2018) tested two full-scale numerical models including all relevant parameters such as geometric and material defects under varying bending moments with experiments on web-tapered steel elements, and summarized the results obtained from each experiment and formed the basis for further studies.

Wang & Nethercot (1990) performed a parametric study addressing bracing requirements for unrestrained beams. For single-bracing systems, authors recommend 1% of axial force in a flange at failure as the bracing-strength requirement. For multiple-bracing systems, a total value of 2% is suggested, with a maximum of 1% for each brace, especially for beams with high slenderness. Lay and Galambos (1966) and Mohammadi et al. (2016) both addressed the design and bracing requirements for steel beams. Lay and Galambos (1966) emphasized the importance of axial strength, axial stiffness, and bending strength in the design of bracing for inelastic steel beams. Mohammadi et al. (2016) studied the brace stiffness requirement additional to the elastic lateral torsional buckling of monosymmetric I-beams under pure bending condition. Both studies provide valuable insights into the factors that need to be considered in the design and bracing of steel beams. Bishop (2013) created a method for calculating inelastic eigenvalue buckling to identify the optimal bracing stiffness needed in general frame systems for metal buildings. He also offered guidelines for the necessary design stiffness and strength of brace components using this calculation tool.

AISC Design Guide 25 (2022) provides comprehensive information on the adequacy of fixed bracing for elements, detailing the critical points to consider in inelastic nonlinear analyses. The guide elaborates on the fixed bracing requirements and calculation methods for symmetrical linearly tapered elements through various examples, and it offers safe calculations for braced points at different unbraced lengths. AISC Design Guide 25 also recommends using computer-aided analysis methods to determine the accuracy and effectiveness of bracing systems. Wijaya et al. (2019) found that AISC Design Guide 25 calculates the critical moment accurately for long beams but not accurately for short beams.

The application of flexible nodal bracing is a common technique to enhance the stability of beams in their transverse direction. The AISC 360-22 (2022) Specification provides simplified design equations for various bracing situations, including “relative” and “nodal” lateral bracing of columns and beams, and “nodal” and “continuous” torsional bracing of beams. According to the AISC guidelines, the brace force demand should typically be within a certain percentage to ensure adequate performance. The inelastic finite element nonlinear analysis used in this study, in light of the operations performed with the finite element method in finite element program, revealed that the brace force demand can increase up to 2.15% instead of the 2% for compact members typically predicted by the AISC. This observed increase should be taken into account in terms of brace stability.

To achieve this result, the compactness of the beam sections was first determined by performing compactness equations mentioned at AISC Appendix 6 Table B4.1b. These calculations allow the identification of the thickness range necessary for the beam to be considered compact. Subsequently, parametric finite element analysis was then used using the selected compact range for flange thickness and web thickness. Considering the complexity of inelastic and nonlinear material behavior, ABAQUS software (Dassault Systèmes / Simulia, 2020) was employed for the finite element analyses. Load proportion factor and node displacement values were obtained from the analyses according to various stiffness values. These parameters were then used to calculate the percentage brace force demand.

The findings of this study may have important implications for the design of mentioned web tapered steel beams; a method may be provided to increase brace force demand to 2.5 %. This article aims to detail the methodology, analysis, and results, providing insights into the practical applications of flexible brace in beam design.

2. Methodology

In this study, a short span welded web-tapered steel beam with a total length of 2540 mm (100in) was used. The 3-d view of beam used is given in Figure 1(a). The material used was ASTM A992 Grade 50 or a similar high-strength structural steel grade. For this steel grade, the modulus of elasticity (E) was taken as 200,000 MPa (29,000 ksi), the yield strength (F_y) as 379.21 MPa (55 ksi), and the tensile strength (F_u) as 547 MPa (79.31 ksi). A flexible nodal brace with variable stiffness was placed at the midpoint of the beam's top flange, dividing the length of the beam in half as shown in Figure 1(b). The height of the beam between top and bottom flanges varies uniformly tapered from 1066.8 mm (42 in) at one end to 924.6 mm (36.4in) at the other end as shown in Figure 1(b). At the point where the brace is located, the web height is 996 mm (39.205 in), and the unbraced length was set to 1270 mm (50in). The flange width is 228.6 mm (9 in).

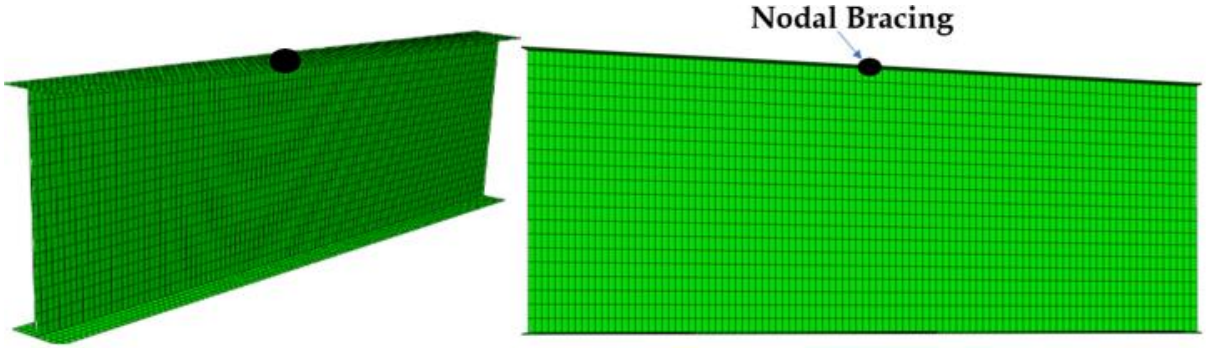

Figure 1. Finite element model of web tapered beam (a) 3-d view and (b) X-Y axis view

The inelastic nonlinear analysis of the beam under an applied moment at the left end was performed as shown in Figure 2(a). The loading condition is described by a moment diagram that forms a right-angled triangle, with the maximum moment at the left end, decreasing towards the right, as shown in Figure 2(b). The inelastic nonlinear analysis of the beam performed within the compact web thickness and flange thickness ranges. First, the compact range for web and flange thickness were calculated according to AISC 360-22 Table B4.1b "Width-to-thickness ratios: Compression elements members subject to flexure". The flange used in this study corresponds to Case 11 of Table B4.1b "flanges of doubly and singly symmetric I-shaped built-up sections" in the table, and the web section corresponds to Case 15 of Table B4.1b "webs of doubly-symmetric I-shaped sections and channels".

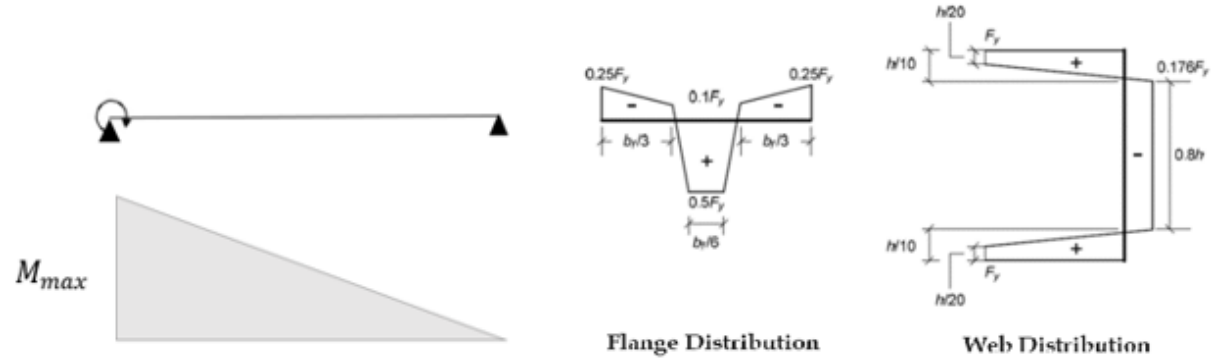

Figure 2. (a) Applied moment illustration, (b) Moment diagram of the beam and (c) Best-Fit Prawel Pattern residual stress (Adapted from Jeong et al. 2016)

For flanges of doubly and singly symmetric I-shaped built-up sections:

$$\frac{b}{t} \leq 0.38\sqrt{\frac{E}{F_y}} = \lambda_P \quad (1)$$

$$\frac{b}{t} \leq 0.95\sqrt{\frac{k_c E}{F_L}} = \lambda_r \quad (2)$$

In the formulas (1) and (2), b corresponds to half of the width of the flange, and t is the thickness of the flange. E means the modulus of elasticity of steel, which is 200,000 MPa (29,000 ksi). F_y means the specified minimum yield stress, which is 379.21 MPa (55 ksi). As given in AISC 360-22 Table B4.1b $k_c = \frac{4}{\sqrt{h/t_w}}$ but shall not be taken less than 0.35 nor greater than 0.76 for calculation purposes, h is the distance between flanges. Similarly, as mentioned in same table, $F_L = 0.7F_y$ for major axis bending of compact and noncompact web built-up I-shaped members with $S_{xt}/S_{xc} \geq 0.7$.

For webs of doubly-symmetric I-shaped sections and channels:

$$\frac{h}{t_w} \leq 3.76\sqrt{\frac{E}{F_y}} = \lambda_P \quad (3)$$

$$\frac{h}{t_w} \leq 0.38\sqrt{\frac{E}{F_y}} = \lambda_r \quad (4)$$

In the formulas (3) and (4), h corresponds to the distance between flanges, and t_w is the thickness of the web section. Again, E means the modulus of elasticity of steel, which is 200,000 MPa (29,000 ksi) and F_y means the specified minimum yield stress, which is 379.21 MPa (55 ksi).

The findings were tabulated in Table 1. Web thicknesses greater than 11.43 mm (0.45 in) and flange thicknesses greater than 13.97 mm (0.55 in) were found to be compact. To obtain results, flange thicknesses between 13.97 mm (0.55 in) and 25.4 mm (1 in) and web thickness ranges between 11.43 mm (0.45 in) and 19.05 mm (0.75 in) were selected within the compact range. Subsequently, for each thickness within this range, inelastic nonlinear analysis was performed using the finite element method by the ABAQUS software (Dassault Systèmes / Simulia, 2020). Since the number of cases is high, Python code written to automate the results and speed up the processes was utilized.

Finite element models of tapered beam cross-sections, with the top flange height tapering from one end to the other, were developed using ABAQUS. The test elements were modeled using a four-node shell element (S4R) for all section components. For all scenarios, the deeper side of the web was exposed to a bending moment. Using Type 1 spring elements in ABAQUS, a single brace was applied at the midspan of the tapered beam, at the top flange height, and connected to the flange-web intersection. The brace stiffness was gradually increased from 0.25 kip/in to 1500 kip/in to reflect the minimum and maximum capacities achievable with a fixed brace. In the study conducted by Lokhande (2014) using Advanced Finite Element Analysis for the strength evaluation of doubly symmetric I-section beams and column-beams, four-node S4R shell elements were used to model the flanges and web of the element while using ABAQUS software.

The shell finite element analysis models integrated residual stresses by employing an existing residual stress pattern (Pattern I). Best-fit Prawel pattern that shown in Figure 2(c) applied in this research. This pattern, valued for its self-equilibrating properties within each component, has been previously utilized by Jeong et al. (2016) for welded cross section.

These imperfection patterns are generated using the geometric imperfection tolerances specified in AWS (2010) and AISC Code of Standard Practice (COSP) (2022). To obtain flange tilt and web out-of-flatness patterns, inelastic eigenvalue buckling analysis is conducted on members with out-of-plane displacements restrained at the top and bottom flange-web juncture points, under uniform axial compression as shown in Figure 3(a). This analysis yields buckling modes, which are then used to isolate and scale the flange tilt and web out-of-flatness patterns to half the tolerance values as has been previously utilized and mentioned by Toğay et al. (2018). Besides the previously discussed imperfections, a flange sweep is introduced at the web-flange juncture points in the Critical Segment (CS). A sinusoidal flange sweep is applied specifically to the top flange, which experiences flexural compression. Conversely, the bottom flange, which is under flexural tension, remains without any sweep, as illustrated in Figure 3(b).

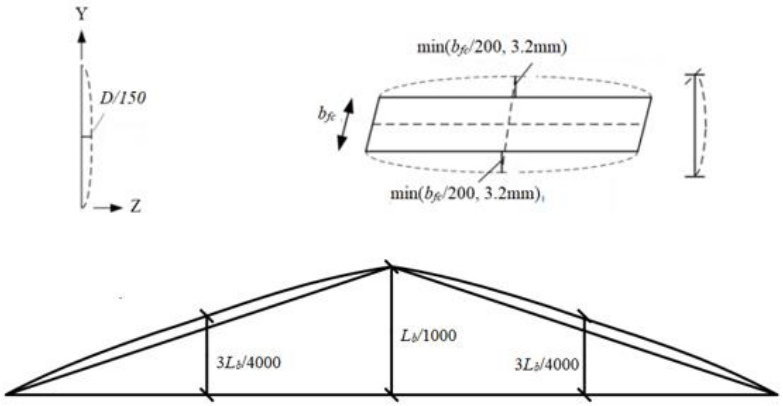

Figure 3. (a) Web out-of-flatness and flange tilt imperfections, and (b) applied imperfections (the AWS/AISC COSP Flange Sweep Tolerance). (Adapted from Toğay and White, 2018)

As a result of these analyses, nodal displacement and load proportionality factor were obtained for a series of stiffness values ranging from 350.25 kN/m (2 kip/in) to 262,690.2 kN/m (1500 kip/in). With these results, compression force at midsection of top flange and brace force were calculated. Then, the brace force was divided by the compression force at midsection of top flange to obtain a percentage value called "brace force demand" for each thickness combination.

Following these calculations, the required brace stiffness was determined according to the procedures outlined in both the AISC 360-22 specification and its commentary. Specifically, it was calculated using the formulas given below under Appendix 6 "Stability Bracing for Beams" Nodal Bracing heading and Commentary Appendix 6 "Stability Bracing for Beams" Lateral bracing heading

Nodal Bracing according to Specification Appendix 6 is;

$$\beta = \frac{10 \times M_r \times C_d}{L_{br} \times h_o \times \Phi} \quad (5)$$

$$P_{rb} = \frac{0.02 \times M_r \times C_d}{h_o} \tag{6}$$

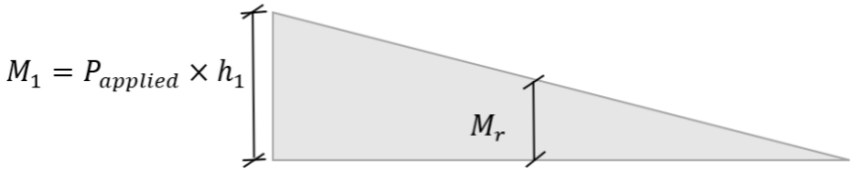

Figure 4. Required flexural strength M_r representation for calculation from moment diagram

$$M_r = \frac{P_{applied} \times h_1 \times (LPF)_{max}}{2} \tag{7}$$

Lateral bracing according to Commentary Appendix 6 is;

$$\beta = \frac{2 \times N_i \times C_t \times P_f \times C_d}{L_{br} \times \Phi} \tag{8}$$

$$P_f = \frac{M_r}{h_o} \tag{9}$$

In the formulas (5), (6), (7), (8), and (9), M_r is required flexural strength using LRFD load combinations at brace point and found from moment diagram shown as Figure 4. C_d is 1 for single curvature bending case, C_t constant is 1 for centroidal loading case. h_o is section height distance between flange centroids in brace point, h_1 is height distance between flange centroids of left side of the beam, and L_{br} is unbraced length and all shown in Figure 5. Φ taken as 1 for performing nominal analysis, P_f is beam compressive flange force, P_{rb} required strength, $P_{applied}$ is applied load and $(LPF)_{max}$ is maximum load proportionality factor found from inelastic nonlinear analysis. For nodal bracing N_i is $= 4 - \frac{2}{n}$ and n is number of braces. Dimensions are illustrated in Figure 5(a) for the side view of the beam and in Figure 5(b) for the front view.

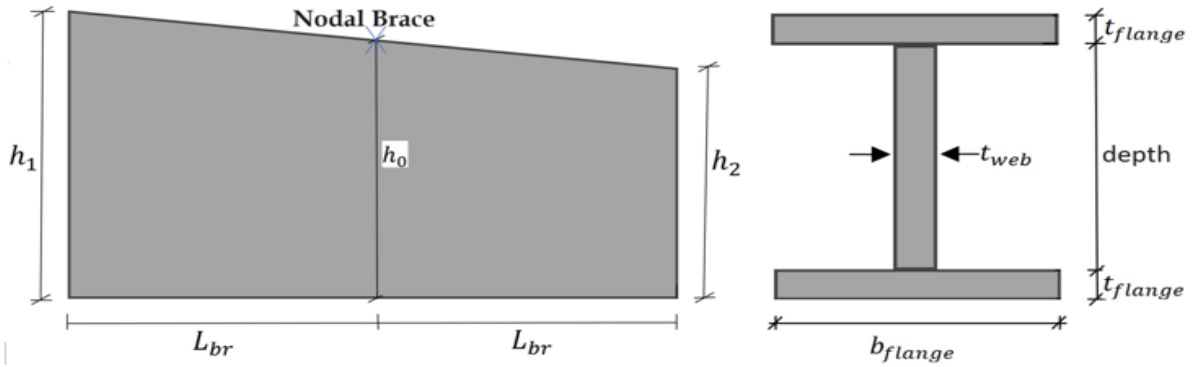

Figure 5. Bracing placement (a) and dimension illustration (b) of section

3. Results

In this section, selected compact thickness ranges are presented for the inelastic nonlinear analysis, which were determined based on the formulas provided in the previous section. The

dimension for flange thickness were chosen to be between 13.97 mm (0.55 in) and 25.4 mm (1 in) as they fall within the compact range. Similarly, the dimension for web thickness were chosen to be between 11.43 mm (0.45 in) and 19.05 mm (0.75 in). The cases studied in the analysis are shown in Table 1.

Table 1. Compact web and flange thickness range

Web thickness (mm)	11.43	12.7	13.97	15.24	16.51	17.78	19.05			
Flange thickness (mm)	13.97	15.24	16.51	17.78	19.05	20.32	21.59	22.86	24.13	25.4

The inelastic nonlinear analysis was performed for each of these thickness combinations using the finite element method with the ABAQUS software. For each flange thickness-web thickness combination, 21 different stiffness values were analyzed individually. The brace force and the compression force at the midsection of the top flange were obtained in all thickness combinations. The required brace force demand was calculated as the ratio of these two forces as mentioned in previous section for all cases. A total of 1470 analyses were conducted, and the results for the required brace force demand for each combination are shown in Table 2.

Table 2. Required brace force percentage demand for sections

%		Flange Thickness (mm)									
		13.97	15.24	16.51	17.78	19.05	20.32	21.59	22.86	24.13	25.4
Web Thickness (mm)	11.43	2.15	2.03	1.98	1.92	1.26	1.85	1.25	1.77	1.74	1.73
	12.7	2.02	1.88	1.83	1.7	1.76	1.75	1.73	1.45	1.31	1.69
	13.97	1.84	1.79	1.73	1.66	1.68	1.73	1.75	1.68	1.77	1.73
	15.24	1.84	1.68	1.69	1.68	1.73	1.65	1.73	1.69	1.77	1.77
	16.51	1.73	1.73	1.79	1.76	1.62	1.64	1.8	1.73	1.67	1.82
	17.78	1.83	1.79	1.75	2.12	1.66	1.8	1.69	1.81	1.75	1.86
	19.05	1.95	1.89	1.52	1.81	1.7	1.57	1.61	1.82	1.77	1.71

To demonstrate, for a specific case with a flange thickness of 25 mm (1 in) and a web thickness of 20 mm (0.75 in), the required brace force demand and brace stiffness values are presented below in Figure 6. The brace stiffness value for Equation (8) is 668 kN/m (41.04 kip/in) and Equation (5) 1670 kN/m (103 kip/in), brace force demand for this case was found as 1.5% and 1.57% respectively.

To illustrate the results for all cases a graph was derived. These graphs represent the results from the ABAQUS analyses conducted for 21 different stiffness values. Same analyses were performed for each case, and the resulting graphs for a specific case shown below. The generated graph demonstrates the relationship between brace stiffness values and the corresponding brace force demand percentage for cases.

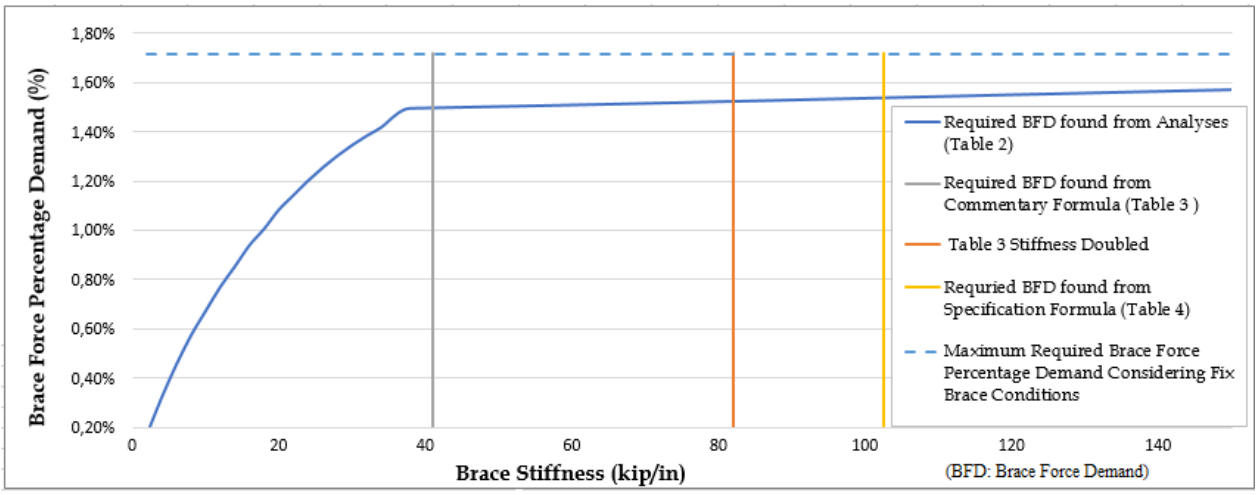

Figure 6. Graph of brace force demand values with respect to stiffness values for example case

As a result of 1470 analyses, brace stiffness values were found for each thickness combination based on the formulas given in previous section. Each of the values shown in Table 3 are the required brace force demand in percentage with respect to beam section brace stiffness values found as a result of the formulas in the AISC commentary mentioned in the methodology.

Table 3. Required brace force percentage demand with respect to brace stiffness values found from Equation (8)

	%	Flange Thickness (mm)									
		13.97	15.24	16.51	17.78	19.05	20.32	21.59	22.86	24.13	25.4
Web Thickness (mm)	11.43	1.98	1.81	1.75	1.69	1.14	1.47	1.1	1.39	1.33	1.34
	12.7	1.87	1.7	1.64	1.56	1.56	1.41	1.34	1.33	1.04	1.34
	13.97	1.74	1.67	1.55	1.56	1.46	1.41	1.41	1.32	1.32	1.3
	15.24	1.7	1.56	1.61	1.55	1.5	1.45	1.41	1.38	1.38	1.34
	16.51	1.65	1.61	1.7	1.61	1.6	1.53	1.53	1.42	1.41	1.41
	17.78	1.75	1.73	1.67	1.55	1.61	1.6	1.56	1.48	1.5	1.47
	19.05	1.88	1.83	1.52	1.79	1.63	1.59	1.54	1.5	1.4	1.5

Correspondingly, the values shown in Table 4 are the required brace force demand in percentage with respect to beam section brace stiffness values found as a result of the formulas in AISC specification Appendix 6 mentioned in the methodology.

Table 4. Required brace force percentage demand with respect to brace stiffness values found from Equation (5)

%		Flange Thickness (mm)									
		13.97	15.24	16.51	17.78	19.05	20.32	21.59	22.86	24.13	25.4
Web Thickness (mm)	11.43	2.12	2	1.99	1.8	1.21	1.64	1.19	1.52	1.41	1.48
	12.7	2	1.88	1.84	1.66	1.6	1.58	1.44	1.41	1.17	1.44
	13.97	1.81	1.8	1.75	1.67	1.58	1.56	1.57	1.42	1.41	1.38
	15.24	1.81	1.64	1.69	1.67	1.62	1.57	1.55	1.43	1.42	1.44
	16.51	1.7	1.72	1.75	1.71	1.61	1.6	1.6	1.58	1.46	1.44
	17.78	1.8	1.79	1.73	1.73	1.64	1.7	1.6	1.56	1.54	1.57
	19.05	1.95	1.84	1.47	1.8	1.69	1.57	1.55	1.56	1.48	1.57

In order to interpret the conducted studies, the brace force demand values obtained from the analysis results initially and presented in Table 2 were compared with the brace force demand values found from brace stiffness values calculated subsequently as mentioned above and shown in Table 3 and Table 4, with the comparison results shown in Table 5. The purpose of this comparison was to observe whether the demands found based on the brace stiffness could meet the values obtained from the section analysis. As a result of this comparison, if the value obtained from the analysis results was greater than the value found based on the brace stiffness, it was shown in the table as red; otherwise, it was shown as light green. In the table, each cell with the intersection of flange thickness-web thickness is divided by 2. While the left part of the divided cells shows the result of comparing Table 2 and Table 3, the right part shows the result of comparing Table 2 and Table 4.

Table 5. Evaluation of Table 2 data in comparison with Table 3 and Table 4 values

Table 3	Table 4	Flange Thickness (mm)									
		13.97	15.24	16.51	17.78	19.05	20.32	21.59	22.86	24.13	25.4
Web Thickness (mm)	11.43										
	12.7										
	13.97										
	15.24										
	16.51										
	17.78										
	19.05										

Note: Flange thicknesses are divided into two, the box on the left is colored according to the comparison of Table 2 with Table 3, and the box on the right side is colored according to the comparison of Table 2 with Table 4.

Based on Table 5 findings, it is observed that as compactness increases in the web elements, the values for maximum brace force percentage demand in Table 2 appear sufficient. Conversely, as compactness decreases for web members, it is found that the brace force percentage demand values corresponding to brace stiffness in Tables 3 and 4 exceed those in Table 2.

Furthermore, while increasing flange thickness does not show a discernible effect, increasing web thickness appears to render the maximum brace force percentage demand values in Table 2 sufficient. These findings illustrate the sensitivity of brace force demands to compactness and the geometric characteristics of structural elements as analyzed in the study.

4. Conclusions

This study has conducted a comprehensive inelastic nonlinear analysis to investigate the brace force demands for various combinations of flange and web thicknesses using the finite element method with ABAQUS software. The findings of this research highlight several key insights into the relationship between brace stiffness values and the corresponding brace force demands.

The analyses revealed that the compactness of web elements significantly impacts the maximum brace force percentage demand. Specifically, as the compactness of web elements increases, the brace force demands derived from the analysis are found to be adequate. Conversely, for less compact web elements, the brace force demands based on the calculated brace stiffness values exceed those obtained from the section analysis.

Additionally, while variations in flange thickness did not demonstrate a significant effect on the brace force demands, an increase in web thickness contributed to achieving sufficient brace force percentage demands. This indicated a notable sensitivity of brace force demands to the compactness and geometric characteristics of the structural elements under consideration.

The results suggest that, for optimal design, attention must be given to the compactness of web elements to ensure that the brace force demands can be met effectively.

Overall, this study contributes to a deeper understanding of the factors influencing brace force demands and provides valuable insights for the design and assessment of structural elements subjected to inelastic nonlinear behavior. Future research could expand on these findings by exploring additional geometric configurations and material properties to further refine the predictive models for brace force demands in structural engineering applications.

Author Statement

The authors confirm contribution to the paper as follows: F. Kömürcü: analysis and interpretation of results, data collection, draft manuscript preparation; O. Toğay: analysis and interpretation of results, draft revision. All authors reviewed the results and approved the final version of the manuscript.

Conflict of Interest

The authors declare no conflict of interest.

References

AISC (2016). *Specification for Structural Steel Buildings,* ANSI/AISC 360-22, American Institute of Steel Construction, Chicago, IL.

AISC (2022). *Specification for Structural Steel Buildings,* ANSI/AISC 360-22, American Institute of Steel Construction, Chicago, IL.

AISC (2022). *ANSI/AISC 303-22: COSP-Code of standard practice for steel buildings and bridges*, American Institute of Steel Construction.

AWS (2010). *Structural Welding Code–Steel*, AWS D1.1: D1.1M, (22nd ed.), prepared by AWS Committee on Structural Welding.

Asgarian, B., Soltani, M., & Mohri, F. (2013). Lateral-torsional buckling of tapered thin-walled beams with arbitrary cross-sections. *Thin-Walled Structures, 62*, 96-108. https://doi.org/10.1016/j.tws.2012.06.007

Bishop, C. D. (2013). *Flange bracing requirements for metal building systems* (Doctoral dissertation, Georgia Institute of Technology). Georgia Institute of Technology.

Dassault Systèmes / Simulia. (2020). *ABAQUS/Standard user's manual version 6.20*. Hibbit, Karlsson & Sorensen Inc.

Foster, A. S. J., & Gardner, L. (2013). Ultimate behaviour of steel beams with discrete lateral restraints. *Thin-Walled Structures*, *72*, 88-101. https://doi.org/10.1016/j.tws.2013.06.009

Jeong, W. Y., Toğay, O., Lokhande, A. M., & White, D. W. (2016). An introspective assessment of buckling and second-order load-deflection analysis based design calculations. In *Proceedings of the Annual Stability Conference*. Structural Stability Research Council. Orlando, FL.

Lay, M. G., & Galambos, T. V. (1966). Bracing requirements for inelastic steel beams. *Journal of the Structural Division*, *92*(2), 53-68. https://doi.org/10.1061/JSDEAG.0001421

Lokhande, A. M. (2014). *Evaluation of steel I-section beam and beam-column bracing requirements by test simulation* (Master's thesis, Georgia Institute of Technology). Georgia Institute of Technology.

Mercuri, V., Balduzzi, G., Asprone, D., & Auricchio, F. (2020). Structural analysis of non-prismatic beams: Critical issues, accurate stress recovery, and analytical definition of the Finite Element (FE) stiffness matrix. *Engineering Structures*, *213*, 110252. https://doi.org/10.1016/j.engstruct.2020.110252

Miller, B. S. (2003). *Behavior of web-tapered built-up I-shaped beams* (Master's thesis). University of Pittsburgh.

Mohammadi, E., Hosseini, S. S., & Rohanimanesh, M. S. (2016). Elastic lateral-torsional buckling strength and torsional bracing stiffness requirement for monosymmetric I-beams. *Thin-Walled Structures*, *104*, 116-125. https://doi.org/10.1016/j.tws.2016.03.009

Soltani, M., Asgarian, B., & Mohri, F. (2019). Improved finite element model for lateral stability analysis of axially functionally graded nonprismatic I-beams. *International Journal of Structural Stability and Dynamics*, *19*(09). https://doi.org/10.1142/S0219455419501086

Soltani, M., & Asgarian, B. (2020). Exact stiffness matrices for lateral–torsional buckling of doubly symmetric tapered beams with axially varying material properties. *Iranian Journal of Science and Technology, Transactions of Civil Engineering.* https://doi.org/10.1007/s40996-020-00402-z

Tankova, T., Martins, J. P., Simões da Silva, L., & Marques, L. (2018). Experimental lateral-torsional buckling behaviour of web tapered I-section steel beams. *Engineering Structures, 168*(4), 168-184. https://doi.org/10.1016/j.engstruct.2018.04.084

Toğay, O. (2018). *Advanced Design Evaluation Of Planar Steel Frames Composed Of General Nonprismatic I-Section Members.* Doctoral Dissertation, School of Civil and Environmental Engineering, Georgia Institute of Technology, Atlanta, GA, 273pp.

Toğay, O. (2024). Application of inelastic nonlinear buckling analysis with stiffness reduction factors to web tapered I sections. *Scientific Research Communications*, *4*(1). https://doi.org/10.52460/src.2024.003

Toğay, O., & White, D. W. (2018, April 10-13). Toward the recognition of unaccounted for flange local buckling and tension flange yielding resistances in the ANSI/AISC 360 specification. In *Proceedings of the Annual Stability Conference* Structural Stability Research Council. Baltimore, Maryland.

Wang, Y. C., & Nethercot, D. A. (1990). Bracing requirements for laterally unrestrained beams. *Journal of Constructional Steel Research*, 17(4), 305-315. https://doi.org/10.1016/0143-974X(90)90078-U

White, D. W., Jeong, W. Y., & Slein, R. (2021). *AISC Design Guide 25: Frame design using nonprismatic members*. American Institute of Steel Construction.

Wijaya, P. K., Swan, C. L., & Noor, G. S. (2019). An analysis of elastic and inelastic lateral torsional buckling of web-tapered I beams using the finite element method. *MATEC Web of Conferences.*